

# Distributed Activation Energy Model of Heterogeneous Coal Ignition

John C. Chen

We present a model that simulates the conventional tube-furnace experiment used for ignition studies. The Distributed Activation Energy Model of Ignition accounts for particle-to-particle variations in reactivity by having a single preexponential factor and a Gaussian distribution of activation energies among the particles. The results show that the model captures the key experimental observations, namely, the linear increase in ignition frequency with increasing gas temperature and the variation of the slope of the ignition frequency with oxygen concentration. The article also shows that adjustments to the model parameters permit a good fit with experimental data.

## NOMENCLATURE

$A_0$	preexponential factor in Arrhenius rate constant of ignition ( $\text{kg m}^{-2} \text{s}^{-1}$ )
$d$	diameter (m)
$E$	activation energy of ignition ( $\text{kJ mol}^{-1}$ )
$E_0$	mean of Gaussian distribution ( $\text{kJ mol}^{-1}$ )
$h$	convective heat transfer coefficient ( $\text{W m}^{-2} \text{K}$ )
$H_c$	heat of reaction ( $\text{J kg}^{-1}$ )
$k$	thermal conductivity ( $\text{W m}^{-1} \text{K}$ )
$n$	reaction order of ignition with respect to oxygen
$Q$	heat generated or heat loss (W)
$R$	universal gas constant ( $8.314 \times 10^{-3} \text{kJ mol}^{-1} \text{K}^{-1}$ )
$S$	external surface area of particle ( $\text{m}^2$ )
$T$	temperature (K)
$y$	molar ratio of CO to $\text{CO}_2$

## Greek Symbols

$\chi_{\text{O}_2}$	oxygen mole fraction at particle surface
$\varepsilon$	emissivity of coal
$\sigma_b$	Stefan-Boltzmann constant ( $5.67 \times 10^{-8} \text{W m}^{-2} \text{K}^{-4}$ )
$\sigma$	standard deviation of Gaussian distribution ( $\text{kJ mol}^{-1}$ )

## Subscripts

conv	convection
g	gas
p	particle
rad	radiation

## INTRODUCTION

Numerous experiments have been conducted over the past three decades to study the ignition of pulverized coals under conditions relevant to utility boilers. The conventional experiment is based on one developed by Cassel and Liebman [1], and consists of a tube furnace containing a heated mixture of  $\text{O}_2$  and inert gas. The temperature of the furnace, and hence the gas, is the independent variable in this arrangement. The experiment is conducted by dropping a small batch of presized coal particles into the hot gas and visually observing for a flash of light, which signals ignition. In such an experiment the particle concentration is typically low enough that each particle can be considered to behave independently of all others. The furnace temperature is then decreased and the experiment is repeated to determine the *minimum gas temperature* (or the *critical gas temperature*) at which ignition occurs. This condition is termed *critical ignition*. Finally, the particle size or the  $\text{O}_2$  concentration is changed and, again, the critical ignition condition is found for the new operating condition.

## THEORY OF HETEROGENEOUS IGNITION

Essenhig et al. [2] describe in detail the theory of heterogeneous ignition, that is, ignition that occurs at the solid-gas interface. For a coal particle exposed to an oxidizing environment, ignition is determined by the balance

between heat generation at and heat loss from the particle surface. The heat loss from the surface of a particle at temperature  $T_p$  is the sum of the losses caused by convection and radiation:

$$Q_{\text{loss}} = Q_{\text{loss, conv}} + Q_{\text{loss, rad}} \\ = hS(T_p - T_g) + \varepsilon\sigma_b S(T_p^4 - T_g^4). \quad (1)$$

Equation 1 assumes that the surroundings involved in radiation exchange are in thermal equilibrium with the gas.

The radiative loss term is relatively unimportant until the particle temperature exceeds  $\sim 1500$  K. For the convective-loss term, we assume that the Nusselt number equals 2, as is appropriate for very small particles, which leads to  $h = 2k_g/d_p$ . Thus, Eq. 1 can be rewritten, on a per-external-surface-area basis, as:

$$\frac{Q_{\text{loss}}}{S} = \frac{2k_g}{d_p}(T_p - T_g) + \varepsilon\sigma_b(T_p^4 - T_g^4). \quad (2)$$

The gas thermal conductivity,  $k_g$ , in the boundary layer around a heated particle is given by a linear fit to the conductivity of air over the temperature range of 300–2000 K:

$$k_g = 7.0 \times 10^{-5} \left[ \frac{T_p + T_g}{2} \right] \frac{\text{W}}{\text{m K}}. \quad (3)$$

Equation 3 represents an approximation for the conductivity evaluated at the mean of the free-stream and particle-surface temperatures, and it is noted that the variation of conductivity with temperature may be represented by higher order representations.

The heat generated by a spherical carbon particle undergoing oxidation on its external

surface is given by the kinetic expression:

$$\frac{Q_{\text{gen}}}{S} = H_c \chi_{\text{O}_2}^n A_0 \exp \left[ \frac{-E}{RT_p} \right]. \quad (4)$$

Diffusion effects are neglected because at the relatively low particle temperatures of pulverized-coal ignition, the oxidation reaction is kinetically controlled.

At the critical ignition condition, the following two conditions are satisfied [2]:

$$Q_{\text{gen}} = Q_{\text{loss}}, \quad (5)$$

$$\frac{dQ_{\text{gen}}}{dT_p} = \frac{dQ_{\text{loss}}}{dT_p}. \quad (6)$$

It is presumed for the purpose of this study that certain of the variables in Eqs. 2 and 4 are known a priori ( $H_c$ ,  $A_0$ ,  $n$ ,  $d_p$ , and  $\varepsilon$ ), or are fixed by the experimental conditions ( $T_g$  and  $\chi_{\text{O}_2}$ ). The values of these variables used for the base case (described below) are shown in Table 1. The remaining unknowns,  $T_p$  and  $E$ , can then be determined by the simultaneous solution of Eqs. 5 and 6; the relation of these two parameters to  $T_g$  for the base case is shown in Fig. 1.  $T_p$  determined in this manner represents the critical ignition temperature, whereas  $E$  can be interpreted as the critical (or maximum) activation energy that a particle may have and still ignite under the given conditions. A detailed expansion of Eqs. 5 and 6 is given in the Appendix.

## MODEL FORMULATION

Figure 2 shows typical data [3] obtained from an ignition experiment conducted by varying the gas temperature while holding all other

TABLE I  
Values of Parameters in the Base Case of the Model

Variable	Value	Units	Remarks
$A_0$	500	$\text{kg m}^{-2} \text{s}^{-1}$	arbitrarily chosen to illustrate model
$d_p$	100	$\mu\text{m}$	arbitrarily chosen to illustrate model
$E_0$	120	$\text{kJ mol}^{-1}$	arbitrarily chosen to illustrate model
$H_c$	9210	$\text{kJ kg}^{-1}$	for the reaction $\text{C} + 1/2 \text{O}_2 \rightarrow \text{CO}$
$n$	1.0	—	arbitrarily chosen to illustrate model
$\sigma$	16.0	$\text{kJ mol}^{-1}$	arbitrarily chosen to illustrate model
$\varepsilon$	0.8	—	arbitrarily chosen to illustrate model

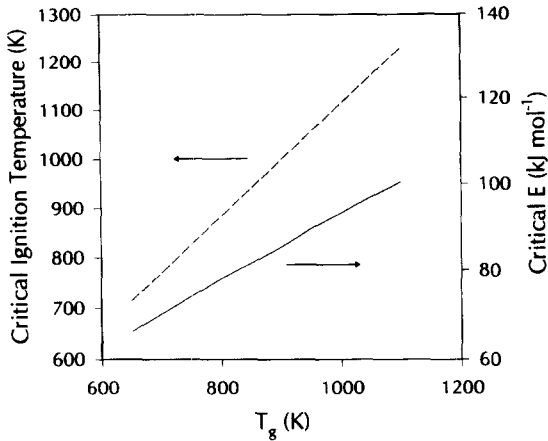


Fig. 1. Relation of critical ignition temperature (dashed line) and critical activation energy (solid line) to gas temperature,  $T_g$ , for base case listed in Table 1.

parameters constant. The data shown was obtained by conducting the experiment as described earlier except that, at each temperature, 10 to 20 tests for ignition were repeated to obtain a frequency or probability of ignition. Fig. 2 shows that ignition frequency increases approximately linearly with gas temperature, and this is inconsistent with the heterogeneous ignition theory previously described. If all particles of a coal sample used in an experiment have the same reactivity, that is, they are de-

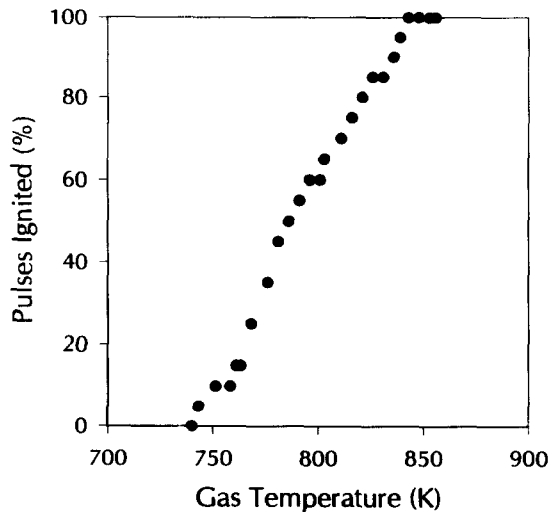


Fig. 2. Typical data from a conventional ignition experiment showing the relation between ignition frequency (or probability) and gas temperature for a bituminous coal. Data extracted from Ref. 3.

scribed by a common Arrhenius rate constant as in Eq. 4, then the data would show an ignition frequency of 0% until the critical gas temperature, corresponding to that at the critical ignition condition, is reached. At any gas temperature above this, the ignition frequency would be 100%. Note that the observed ignition frequency trend is not an artifact of the experiment; this same behavior is reported from a variety of ignition experiments [4, 5, 6] including thermogravimetric analyzers and laser-based studies.

One of the reasons why ignition frequency should increase gradually with increasing gas temperature is somewhat obvious: Within any sample of coal, there exists a *distribution of reactivity* among the particles. Thus, in the conventional ignition experiment, in which a batch of perhaps a few hundred particles of a sample is dropped into the furnace, there is an increasing probability (or frequency) that at least one particle has a reactivity that meets or exceeds the critical ignition condition set forth in Eqs. 5 and 6 as the gas temperature is increased. Of course, there exist other variations among the particles within a sample, such as particle size and specific heat. Variation in size alone could account for the observed increase in ignition frequency with gas temperature. It cannot account for another experimental observation, however, namely the variation in the slope of the ignition frequency with oxygen concentration. (This behavior is described in a later section.) A distribution in specific heat would only affect the rate at which a particle attains its equilibrium temperature, but would not change this value or the reactivity. Perhaps other variations could cause the observed behavior of ignition frequency. It is our premise that the distribution in reactivity dominates all other variations, however, and therefore accounts for the observed behavior.

The Distributed Activation Energy Model of Ignition (DAEMI) models the conventional ignition experiment by allowing for the particles within the coal sample to have a distribution of reactivity. We prescribe that all the particles have the same properties, including the pre-exponential factor in the Arrhenius rate constant describing their ignition reactivity, and that their activation energy is distributed according

to the Gaussian (or normal) distribution:

$$f(E) = \frac{1}{(2\pi\sigma^2)^{0.5}} \exp\left[-\frac{(E - E_0)^2}{2\sigma^2}\right] \quad (7)$$

where  $E_0$  is the mean and  $\sigma$  is the standard deviation of the distribution. The expression

$$\int_E^{E+\Delta E} f(E) dE \quad (8)$$

describes the frequency or probability that particles within a sample have an activation energy in the range  $E$  to  $E + \Delta E$ . Accordingly, the distribution satisfies the condition that  $\int_{-\infty}^{\infty} f(E) dE = 1$ .

The DAEMI divides a prescribed distribution into discrete energy intervals of  $\Delta E = 3$  kJ mol<sup>-1</sup>, and considers only the energy range of  $E_0 - 3\sigma$  to  $E_0 + 3\sigma$ , rather than  $-\infty$  to  $+\infty$ . The latter simplification still covers 99.73% of the distribution. The model then calculates the frequency of being in each of these intervals by numerically integrating Eq. 8 for each of the intervals.

An ignition experiment is modeled by assuming that 10<sup>5</sup> particles are in the initial sample, and that they are distributed among the various  $\Delta E$  intervals according to the calculated frequency for each interval. Each simulation of an experimental run under a given set of conditions is conducted on a batch of 100 randomly selected particles from the sample, keeping in mind that no particle can be selected more than once. Whether or not ignition occurs for a run is determined by the particle in the batch of 100 with the lowest activation energy. If this particle's reactivity equals or exceeds that determined by the critical ignition condition (that is, its activation energy is less than or equal to the critical energy determined by solution of Eqs. 5 and 6), the batch is defined as ignited. This is consistent with our observation [6] that single-particle ignition is discernible to the eye, and certainly to a photon detector. This procedure is repeated 20 times at each condition, just as in actual experiments, to determine an ignition frequency at this condition. Finally, the gas temperature is varied several times and, each time, 20 runs are conducted.

## RESULTS AND DISCUSSION

Figure 3 shows model results of ignition frequency versus gas temperature for one hypothetical sample for which  $E_0 = 120$  kJ mol<sup>-1</sup>,  $\sigma = 16$  kJ mol<sup>-1</sup>, and  $A_0 = 500$  kg m<sup>-2</sup> s<sup>-1</sup>. The other parameters of this base case calculation are listed in Table 1. It is obvious that the DAEMI exhibits the experimental characteristic of increasing ignition frequency with increasing gas temperature. As stated earlier, this is expected as an increase in gas temperature leads to an increase in the maximum activation energy that a particle can have and still be ignitable (see Fig. 1), and therefore to an increased probability of having at least one particle within each batch of a simulated run that is reactive enough to ignite.

Figures 4 and 5 display the effects of varying  $E_0$  and  $\sigma$ , respectively, on the DAEMI. An increase in  $E_0$ , which shifts the Gaussian distribution to higher energies (Fig. 4a), has the effect of shifting the ignition-frequency data to higher gas temperatures (Fig. 4b). This is the expected behavior as a representative batch from the higher  $E_0$  sample contains, on average, particles with higher activation energies, which require a higher temperature to induce ignition. Note that  $E_0$  has only a slight effect on the slope of the data in Fig. 4b.

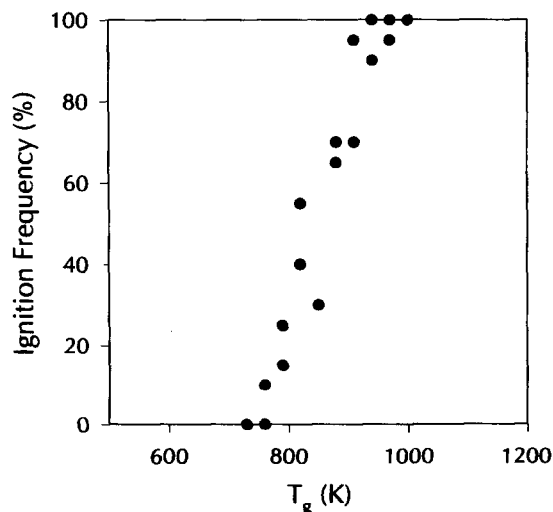


Fig. 3. Results from Distributed Activation Energy Model of Ignition (DAEMI) for base case (Table 1).

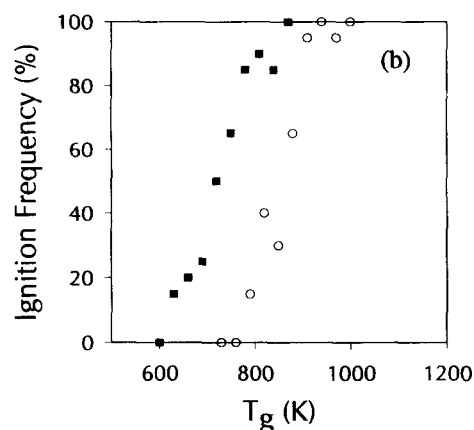
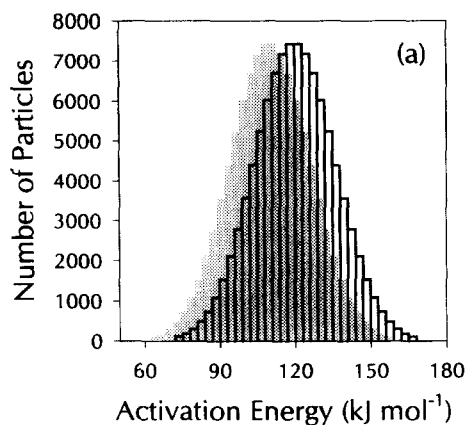


Fig. 4. DAEMI results showing the effect of  $E_0$  on ignition frequency. (a) Solid-colored distribution corresponds to  $E_0 = 110 \text{ kJ mol}^{-1}$ , and the distribution shown in outline corresponds to  $E_0 = 120 \text{ kJ mol}^{-1}$ ; all other parameters are as listed in Table 1. (b) Ignition frequency data for  $E_0 = 110 \text{ kJ mol}^{-1}$  (■) and  $E_0 = 120 \text{ kJ mol}^{-1}$  (○).

Figure 5 shows that an increase in the standard deviation ( $\sigma$ )—the spread of the Gaussian distribution (Fig. 5a)—has two effects: a shift of the ignition frequency to lower temperatures and a slower rise of ignition frequency with gas temperature (Fig. 5b). These findings are somewhat unexpected because the average activation energy ( $E_0$ ) is the same for both samples, and they result from the use of a small batch (100 particles) in each run. The shift to lower temperatures is caused by the fact that, statistically, the most reactive particle in the larger  $\sigma$  batch will have a lower activa-

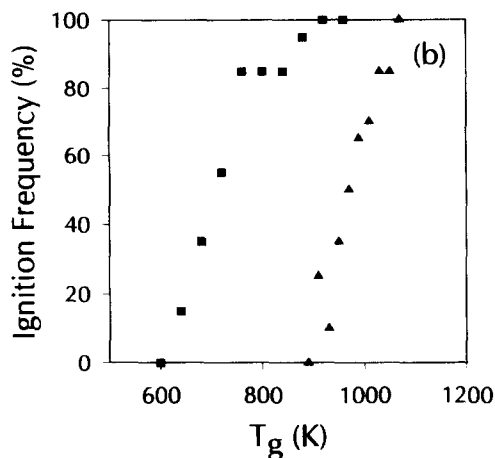
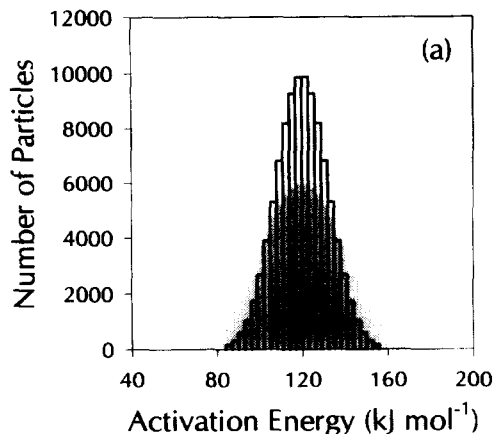


Fig. 5. DAEMI results showing the effect of  $\sigma$  on ignition frequency. (a) Solid-colored distribution corresponds to  $\sigma = 20 \text{ kJ mol}^{-1}$ , and the distribution shown in outline corresponds to  $\sigma = 12 \text{ kJ mol}^{-1}$ ; all other parameters are as listed in Table 1. (b) Ignition frequency data for  $\sigma = 20 \text{ kJ mol}^{-1}$  (■) and  $\sigma = 12 \text{ kJ mol}^{-1}$  (▲).

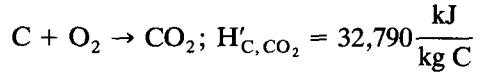
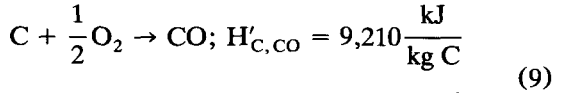
tion energy than the most reactive particle from the smaller  $\sigma$  batch because of its wider spread in distribution. Thus, the higher reactivity allows for ignition to occur at lower temperatures. The wider spread and small batch also cause the slower approach to 100% ignition frequency because the probability of having a batch containing only relatively higher energy particles is increased, which requires higher gas temperatures until all runs result in ignition. Clearly, by adjusting the two parameters of the Gaussian distribution (Eq. 7),  $E_0$  and  $\sigma$ , the DAEMI can be fitted to ignition data, such as those in Fig. 2, provided that accurate val-

ues for the parameters shown in Table 1 are available.

The DAEMI in its present form fails to capture a second experimental characteristic, namely, the change in slope of the ignition frequency data with oxygen concentration, as shown in Fig. 6. The lines shown are linear regressions of experimental data from Ref. 3. (The data points are explained below.) In fact, the DAEMI shows a very weak dependence on oxygen concentration (not shown), so the question remains as to what parameter has not

been or is incorrectly accounted for. The obvious candidate is the reaction order,  $n$ , which must vary with  $\chi_{O_2}$  in order to cause the observation. We can think of no fundamental basis for this behavior, however.

A second, less obvious parameter is the heat of reaction,  $H_c$ , of ignition. So far in the presentation of the DAEMI, it has been assumed that the product of coal ignition is CO, as shown by the value for  $H_c$  in Table 1. It is well known that the product of carbon oxidation is both CO and CO<sub>2</sub>, however, with the relative amounts dependent on both temperature and oxygen partial pressure [7, 8]. The significance of this is that their heats of reaction are vastly different:



Thus, the value of  $H_c$  in Eq. 4 is dependent on the relative amounts of CO and CO<sub>2</sub> formed during ignition, and is given by the expression:

$$H_c = \frac{y}{y+1} H'_{c,CO} + \frac{1}{y+1} H'_{c,CO_2}, \quad (10)$$

where  $y = \text{mol CO/mol CO}_2$ . We have assumed here that energy released by any CO that oxidizes as it diffuses away from the particle surface does not affect the ignition.

This modification to the DAEMI should now show the experimental trend. Measurements [7, 8] show that at higher particle temperature (which results from higher  $T_g$ ), the molar ratio CO/CO<sub>2</sub> increases and consequently  $H_c$ , the amount of heat released during ignition, decreases. Therefore, the result of a set of runs conducted at a decreased oxygen level not only shifts the ignition frequency data to a higher  $T_g$  (a direct result of the decreased  $\chi_{O_2}$ ) but also reduces the slope of the rise (an indirect result because of the decreased  $H_c$ ).

Direct measurements of the CO/CO<sub>2</sub> ratio have been made by Du et al. [7] in a thermogravimetric analyzer (TGA) using soot as the carbon material. Measurements were made over the temperature range of 667–873 K and

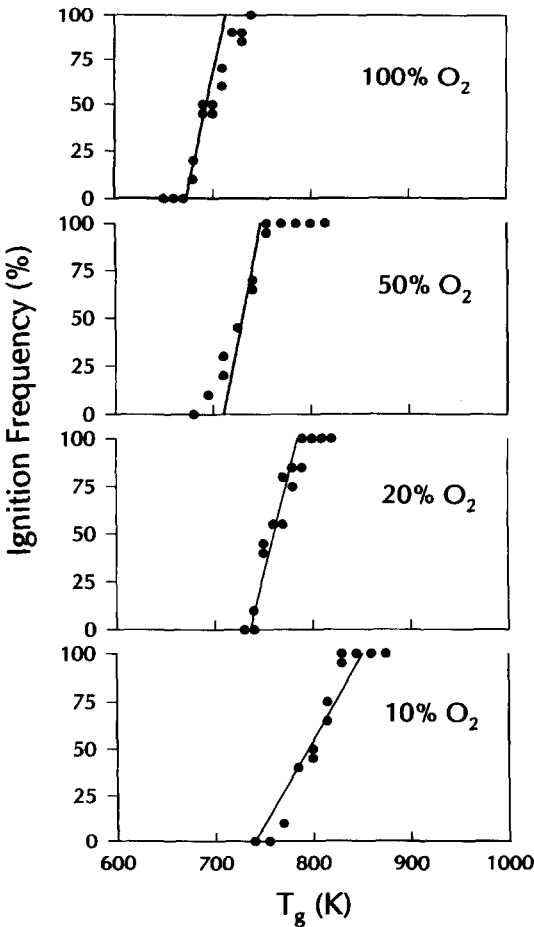


Fig. 6. Linear regressions of experimental data from Ref. 3 (shown as solid lines), showing the effect of free-stream oxygen concentration on ignition of a high-volatile bituminous coal of diameter 75–90  $\mu\text{m}$ . The data points represent results from the DAEMI, including the modification to account for the production of both CO and CO<sub>2</sub> and adjustments to the base case values for  $E_0$ ,  $\sigma$ , and  $n$ , as described in the text.

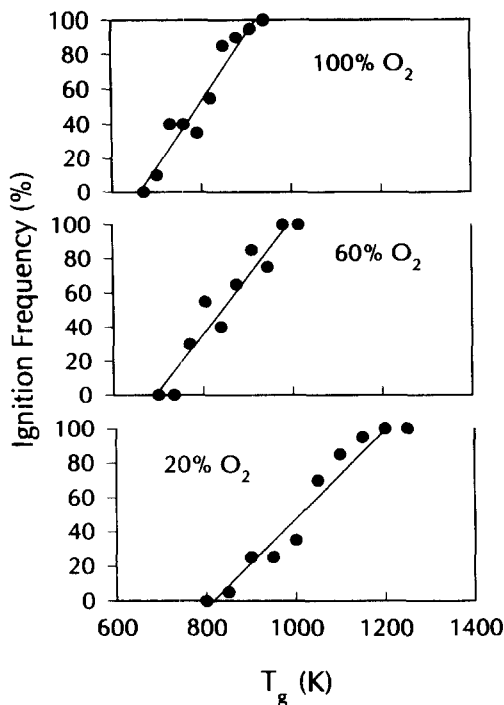


Fig. 7. DAEMI results, including the modification to account for the production of both CO and CO<sub>2</sub>, showing the effect of oxygen concentration on ignition frequency. The solid lines indicate linear regressions of the data points.

oxygen partial pressures from 0.1 to 1 atm. The results at an oxygen partial pressure of 0.21 atm are correlated by the expression:

$$\frac{\text{mol CO}}{\text{mol CO}_2} = 59.95 \exp\left[\frac{-3214}{T_p(\text{K})}\right] \quad (11)$$

This correlation is incorporated into the DAEMI and the model results are shown in Fig. 7. Notice that the model now clearly possesses the desired characteristic. Furthermore, it captures *both* the decrease in the slope of the ignition frequency with decreasing oxygen concentration, and the slow rate of the slope's decrease until low oxygen concentrations, showing the nonlinear behavior with  $\chi_{\text{O}_2}$  displayed in experimental data (Fig. 6).

By adjusting the mean, the standard deviation and the reaction order,  $n$ , of the base case, this current version of DAEMI can be fit to the experimental data shown in Fig. 6. (The particle diameter has also been changed to

83.0  $\mu\text{m}$  to match the mean of the sample used in Ref. 3.) The model results using  $E_0 = 84.0 \text{ kJ mol}^{-1}$ ,  $\sigma = 4.0 \text{ kJ mol}^{-1}$ , and  $n = 0.4$ , are plotted as data points in Fig. 6 over the regression lines and show that a satisfactory fit is achieved with minimal effort in parameter adjustment, despite the uncertainties in the values of other parameters. (Because of the small value of  $\sigma$  used, the energy intervals into which the distribution is divided was decreased from  $3 \text{ kJ mol}^{-1}$  to  $1 \text{ kJ mol}^{-1}$  to obtain these results.) It should be noted that the ignition parameters reported above represent merely a rough fit to the experimental data; it is certainly possible that another set of parameters can also fit the data satisfactorily, especially if a different value for  $A_0$  were chosen. This extra effort may be worthwhile as certain parameters have strong theoretical justification (the reaction order,  $n$ , for example) for being within a particular range. We have begun work to examine this issue in more detail.

Although we have assumed in this study that pulverized-coal ignition occurs heterogeneously without influence from any volatile matter that may be present, and even though the results closely fit the experimental data, it cannot be said that the DAEMI confirms that ignition is purely a heterogeneous process. Very few models of homogeneous ignition have been presented, and none have been tested against the available experimental data because of the inherent difficulty and uncertainty in modeling devolatilization and the combined solid- and gas-phase reactions.

## CONCLUSIONS

The DAEMI has been formulated to model conventional coal-ignition experiments. It accounts for particle-to-particle variations in reactivity within a sample by allowing for a distribution in activation energies among the particles and a single preexponential factor.

The model captures the main characteristics of actual experiments: the gradual increase in ignition frequency with increasing gas temperature and the variation of the slope of the ignition frequency with O<sub>2</sub> concentration. Finally, it has been shown that adjustments to the model parameters can be used to fit experi-

mental data and extract reaction rate constants.

The support of the U.S. Department of Energy (Grant DE-FG22-94MT94013) for this project is gratefully acknowledged.

## REFERENCES

1. Cassel, H. M., and Liebman, I. *Combust. Flame* 3:467–475 (1959).
2. Essenhigh, R. H., Mahendra, K. M., and Shaw, D. W., *Combust. Flame* 77:3–30 (1989).
3. Zhang, D., Wall, T. F., Harris, D. J., Smith, I. W., Chen, J., and Stanmore, B. R., *Fuel* 7:1239–1246 (1992).
4. Tomeczek, J., and Wojcik, J., *Twenty-Third Symposium (International) on Combustion*, The Combustion Institute, Pittsburgh, 1990, pp. 1163–1167.
5. Boukara, R., Gadiou, R., Gilot, P., Delfosse, L., and Prado, G., *Twenty-Fourth Symposium (International) on Combustion*, The Combustion Institute, Pittsburgh, 1993, pp. 1127–1133.
6. Chen, J., Taniguchi, M., Narato, K., and Ito, K., *Combust. Flame* 97:107–117 (1994).
7. Du, Z., Sarofim, A. F., and Longwell, J. P., *Energy and Fuels* 5:214–221 (1991).
8. Mitchell, R. E., Kee, R. J., Glarborg, P., and Coltrin, M. E., *Twenty-Third Symposium (International) on Combustion*, The Combustion Institute, Pittsburgh, 1990, pp. 1169–1176.

Received 30 July 1995; accepted 4 February 1996

## APPENDIX

### Expansion of Eqs. 5 and 6

In order to determine the critical ignition temperature of the particle,  $T_p$ , and critical activation energy,  $E$ , Eqs. 5 and 6 are solved simultaneously.  $Q_{gen}$  and  $Q_{loss}$  are given in Eqs. 2 and 4, and lead to the following derivatives with respect to temperature:

$$\frac{dQ_{gen}}{dT_p} = SH_c \chi_{O_2}^n A_0 \exp\left[\frac{-E}{RT_p}\right] \left(\frac{E}{RT_p^2}\right) \quad (12)$$

$$\frac{dQ_{loss}}{dT_p} = \frac{2k_g}{d_p} S + 4\epsilon\sigma_b S T_p^3. \quad (13)$$

Note that the neglect of the  $T_p$  dependence in  $k_g$  introduces a small error in Eq. 13.

Following Eq. 6, we set Eq. 12 equal to Eq. 13 and solve for the quantity  $E/RT_p$ :

$$\frac{E}{RT_p} = \frac{\frac{2k_g}{d_p} T_p + 4\epsilon\sigma_b T_p^4}{H_c \chi_{O_2}^n A_0 \exp\left[\frac{-E}{RT_p}\right]}. \quad (14)$$

The denominator is recognized to be  $Q_{gen}/S$  (Eq. 4), which by Eq. 5 is also  $Q_{loss}/S$  (Eq. 2). Thus Eq. 14 can be rewritten as:

$$\frac{E}{RT_p} = \frac{\frac{2k_g}{d_p} T_p + 4\epsilon\sigma_b T_p^4}{\frac{2k_g}{d_p} (T_p - T_g) + \epsilon\sigma_b (T_p^4 - T_g^4)}. \quad (15)$$

This relation for  $E/RT_p$  is substituted into the expression  $Q_{gen} - Q_{loss} = 0$  to obtain a function,  $F$ , which is a function of  $T_p$  only:

$$\begin{aligned} F(T_p) &= Q_{gen} - Q_{loss} \\ &= H_c \chi_{O_2}^n A_0 \\ &\quad \times \exp\left[\frac{-\frac{2k_g}{d_p} T_p - 4\epsilon\sigma_b T_p^4}{\frac{2k_g}{d_p} (T_p - T_g) + \epsilon\sigma_b (T_p^4 - T_g^4)}\right] \\ &\quad - \frac{2k_g}{d_p} (T_p - T_g) - \epsilon\sigma_b (T_p^4 - T_g^4) = 0. \end{aligned} \quad (16)$$

The reasonable root of  $F(T_p)$  corresponds to the critical ignition temperature of the particle, and substitution of this value into Eq. 15 produces the critical activation energy at the critical ignition condition.